TENTH AUSTRALASIAN FLUID MECHANICS
CONFERENCE - UNIVERSITY OF MELBOURNE
11-15 DECEMBER 1989

THREE-DIMENSIONAL BOUNDARY LAYER FLOW WITH STREAMWISE ADVERSE PRESSURE GRADIENT

David M. DRIVER[1] and James P. JOHNSTON[2]

[1] NASA Ames Research Center M/S 229-1
Moffett Field, CA 94035 USA

[2]Department of Mechanical Engineering
Stanford University, Stanford CA 94305 USA

ABSTRACT

The effects of a strong adverse pressure gradient ($\frac{\delta^*}{\tau}\frac{\partial P}{\partial x} \approx 12$) on a three-dimensional turbulent boundary layer are studied in an axisymmetric spinning cylinder geometry. Velocity measurements made with a three-component laser Doppler velocimeter include all three mean flow components, all six Reynolds stress components, and all ten triple-product correlations. Total Reynolds shear stress, $\sqrt{\overline{uv}^2 + \overline{vw}^2}$, diminishes as the flow becomes three-dimensional. Lower levels of shear stress were seen to persist under adverse pressure gradient conditions. This low level of stress was seen to roughly correlate with the magnitude of crossflow (relative to free-stream flow) for this experiment as well as most of the other experiments in the literature. Variations in pressure gradient do not appear to alter this correlation. For this reason, it is believed that a three-dimensional boundary layer is more prone to separate than a two-dimensional boundary layer, although it could not be directly shown here.

INTRODUCTION

Boundary layer flow over swept wings, fuselages, and turbine rotor blades often experience extra rates of strain due to pressure gradient and mean flow skewing (three-dimensionality). Turbulence can be greatly affected by these extra rates of strain, and consequently models for turbulence need to be sensitive to these effects. While the effects of individual strain rates on the turbulence are becoming better known via experiment, the effects of combined strain-rates are less well known.

Experimental observations of Reynolds shear stress in three-dimensional (3D) boundary layer flows by Bradshaw & Pontikos (1985) and Driver & Hebbar (1987) suggest that the Reynolds shear stress levels decrease with increasing transverse strain. These observations suggest that a 3D boundary layer may be more prone to separate than a 2D boundary layer, because the boundary layer relies on the Reynolds shear stress (turbulent mixing) to maintain forward flow near the wall in the face of an adverse pressure gradient. The usual reaction of a boundary layer to an adverse pressure gradient is an increase Reynolds shear stress in the middle of the boundary layer (see Simpson, Chew, & Shivaprasad (1981)), thus building further resistance to separation. However, if Reynolds shear stress is reduced by transverse strain, the boundary layer should become less capable of surviving an adverse pressure gradient without separating.

The 3D mild adverse pressure gradient flow of Bradshaw & Pontikos (1985) ($\frac{\delta^*}{\tau}\frac{\partial P}{\partial x} < 2.5$) exhibits a decrease in Reynolds shear stress associated with transverse strain. The object of this study is to assess the effects of a strong adverse pressure gradient ($\frac{\delta^*}{\tau}\frac{\partial P}{\partial x} \approx 12$) on a 3D boundary layer, with the intent of improving turbulence modeling.

In this experiment, a 3D boundary layer is created by passing flow over a laterally translating wall (spinning cylinder aligned with flow). The lateral wall translation produces a transverse strain rate ($\partial W/\partial y$) in addition to the usual streamwise strain rate ($\partial U/\partial y$). An adverse pressure gradient is imposed on the flow by virtue of tunnel wall divergence.

EXPERIMENT

The experiment was conducted in a 31 x 31-cm low-speed (U_r=30 m/s) wind tunnel with a 14-cm-diameter cylinder running the length of the tunnel along the tunnel centerline (Fig. 1). The middle segment of the cylinder was rotated with a surface speed (W_s) of 30 m/s to produce a transverse flow in the boundary layer. Most measurements were performed downstream of the spinning cylinder on a stationary section of cylinder where the transverse flow is relaxing back to an axially aligned flow. An adverse pressure gradient is imposed on the cylinder ($\frac{\delta^*}{\tau}\frac{\partial P}{\partial x} \approx 12$) as a result of tunnel wall divergence, which begins at the end of the rotating section. On the downstream stationary segment of cylinder, the boundary layer is reacting to both the sudden change in boundary condition (the cessation of spin) and the adverse pressure gradient. The boundary layer thickness at the end of the rotating section was 2.8 cm with a momentum-thickness Reynolds number of 6000. The experiment is described in detail in Driver and Johnston (1989).

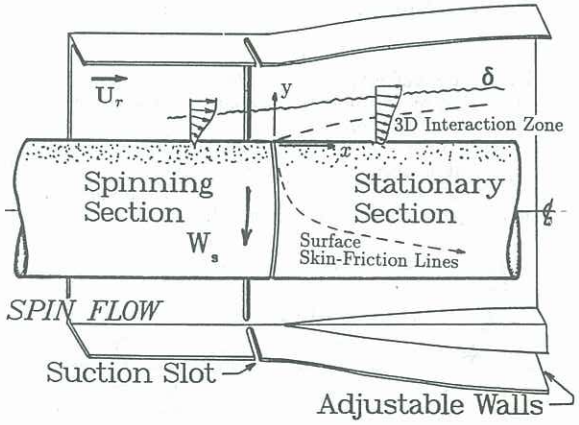

Figure 1 Spinning cylinder test geometry.

The six Reynolds stresses, including all ten velocity triple-product correlations, were measured with a three-component laser Doppler velocimeter (LDV). Uncertainties in U,V and W were estimated to be ±1%. Uncertainties in $\overline{u^2}$, $\overline{v^2}$, and $\overline{w^2}$ were estimated to be ±10% while uncertainties in $\overline{uv}$, $\overline{vw}$, and $\overline{uw}$ were estimated to be ±5% of $\sqrt{\overline{u^2}\,\overline{v^2}}$, $\sqrt{\overline{v^2}\,\overline{w^2}}$ and $\sqrt{\overline{u^2}\,\overline{w^2}}$ respectively. Velocity triple-product correlations $\overline{u_i u_j u_k}$ were calculated with accuracies of ±5% of $\sqrt{\overline{u_i^2}\,\overline{u_j^2}\,\overline{u_k^2}}$. Surface skin-friction was measured with a laser oil-flow interferometer with accuracies of ±10% of local value, and surface static pressure was measured to ±1% of reference dynamic pressure.

RESULTS AND DISCUSSION

Three cases were studied: 1) an adverse pressure gradient with cylinder spinning (case D.S1), 2) zero pressure gradient with spin (case A.S1), and 3) adverse pressure gradient without spin (case D.S0). The first case (case D.S1) is of primary interest, since it contains the combined effects of adverse pressure gradient and three-dimensionality. The other cases are given for comparison. Each case was surveyed in detail at 12 axial stations using a three-component LDV.

The axial component of mean velocity for case D.S1 becomes significantly retarded with distance X along the pressure gradient (see Fig. 2). The flow remains attached with the shape factor (δ_x^*/θ_{xx}) growing to 1.75 at the downstream station. The Clauser parameter $(\frac{\delta^*}{\tau_w}\frac{\partial P}{\partial x})$ grows to $\approx$ 12 by X=100 mm and stays constant thereafter, indicating that this is a severe pressure gradient by most standards.

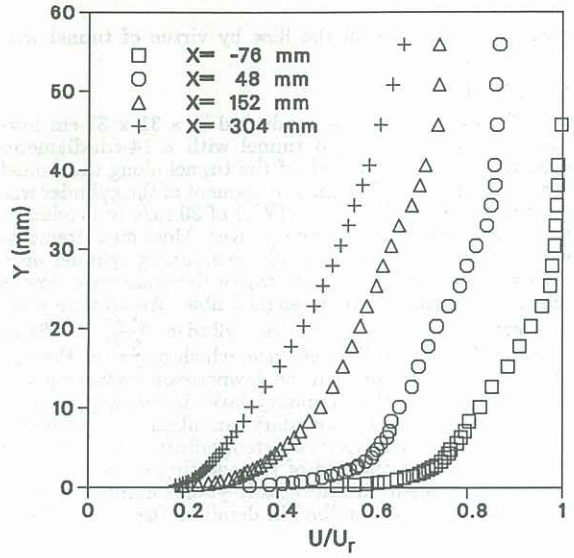

Figure 2 Axial velocity profiles.

Transverse velocity for the adverse pressure gradient case (indicated by symbols) is compared to the corresponding zero pressure gradient case (indicated by lines) in Figure 3. Upstream, near the surface of the spinning cylinder, the W component is large, extrapolating to the surface speed of the cylinder for $y \to 0$. Downstream, the W velocity component decays with distance along the stationary section of the cylinder. The region of diminished W velocity is initially confined to a area near the wall which expands outward toward the boundary layer edge with distance downstream. This region is referred to as the 3D interaction zone. The adverse pressure gradient case shows more decay of W velocity than does the zero pressure gradient case, because of greater boundary layer spreading and diffusion of transverse (angular) momentum to regions further away from the wall.

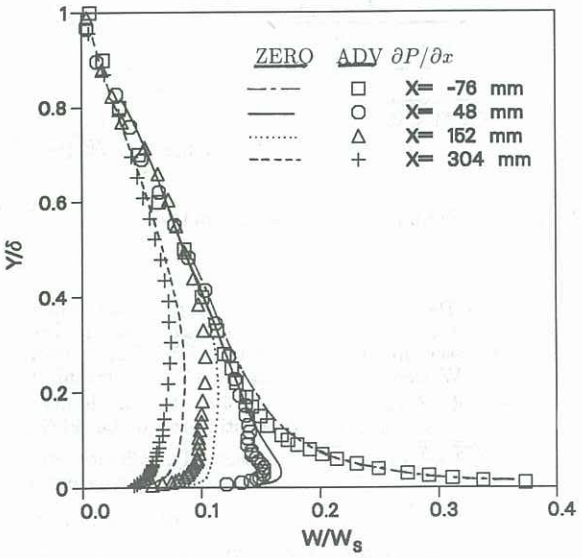

Figure 3 Transverse velocity profiles.

Shear Stress Reduction Phenomenon

Measured distributions of $-\overline{uv}$ and $\overline{vw}$ Reynolds shear stresses are shown in Figures 4 and 5 for adverse $\partial P/\partial x$ case (indicated by symbols) and zero $\partial P/\partial x$ case (indicated by lines). On the spinning cylinder, the profiles of $-\overline{uv}$ and $\overline{vw}$ stress appear very similar to one another and similar to a 2D shear stress distribution. Downstream on the stationary section, the similarity ends; while $\overline{vw}$ stress becomes negative near the wall, $-\overline{uv}$ stress remains positive. The

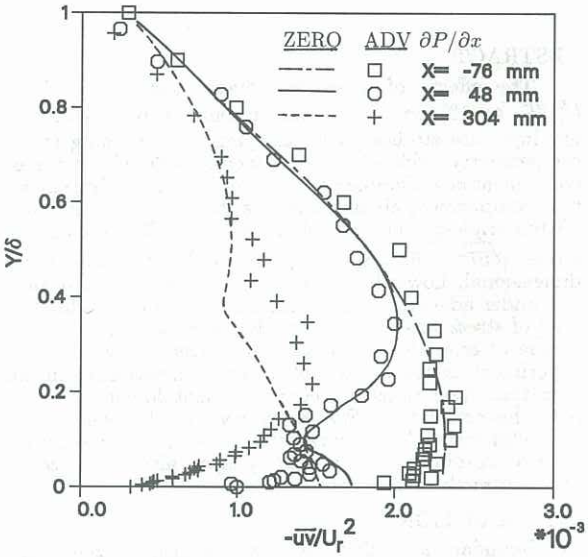

Figure 4 $-\overline{uv}$ Reynolds shear stress.

$-\overline{uv}$ stress decreases in magnitude with distance along the stationary cylinder, due in part to the mean flow three-dimensionality. The reduction in $-\overline{uv}$ stress is also due to a drop in turbulent kinetic energy production associated with the removal of transverse strain. Calculations using a

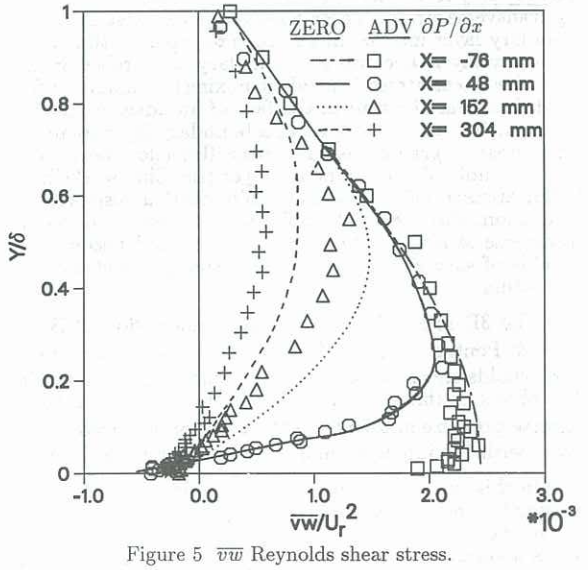

Figure 5 $\overline{vw}$ Reynolds shear stress.

Launder, Reece, & Rodi (1975) full Reynolds stress turbulence model and a Wilcox & Rubesin (1980) $k-\omega^2$ model are shown in Figure 6a, showing the failure of these models to predict this reduction in $-\overline{uv}$ stress, despite the model's ability to predict the corresponding 2D adverse $\partial P/\partial x$ case as shown in Figure 6b. The mixing length model (not shown) separates at X=120 mm in the spinning case, thus ending the calculation before the X=152 mm station. Compared to zero pressure gradient (indicated by lines), the adverse pressure gradient decreases the $-\overline{uv}$ shear stress near the wall and increases it away from the wall as shown in Figures 4 and 5.

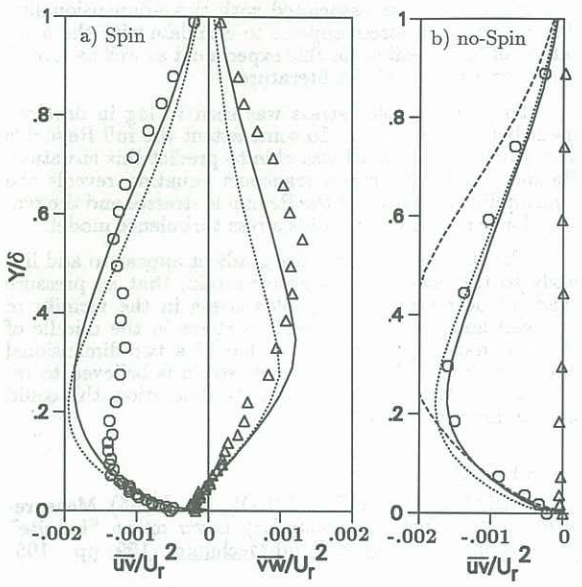

Figure 6 Calculated Reynolds shear stresses at X=152 mm. —— LRR, ····· $k-\omega^2$, – – – Mixing Length.

The ratio $\sqrt{\overline{uv}^2+\overline{vw}^2}$ to twice the kinetic energy (q^2) is also lower than expected ($\sqrt{\overline{uv}^2+\overline{vw}^2}/q^2$=0.15 for 2D flow) as shown in Figure 7. This reduced level of $\sqrt{\overline{uv}^2+\overline{vw}^2}/q^2$ is characteristic of 3D mean flows in general. Furthermore, the magnitude of $\sqrt{\overline{uv}^2+\overline{vw}^2}/q^2$ (at y=.1δ) appears to roughly correlate with the magnitude of crossflow (relative to free stream flow) as shown in Figure 8.

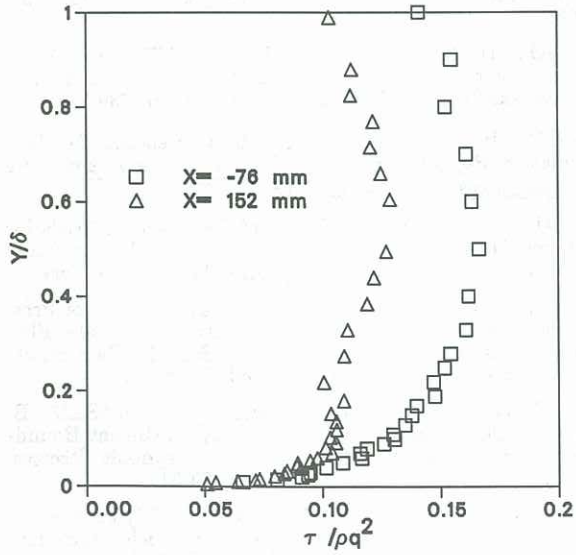

Figure 7 Structure parameter distribution.

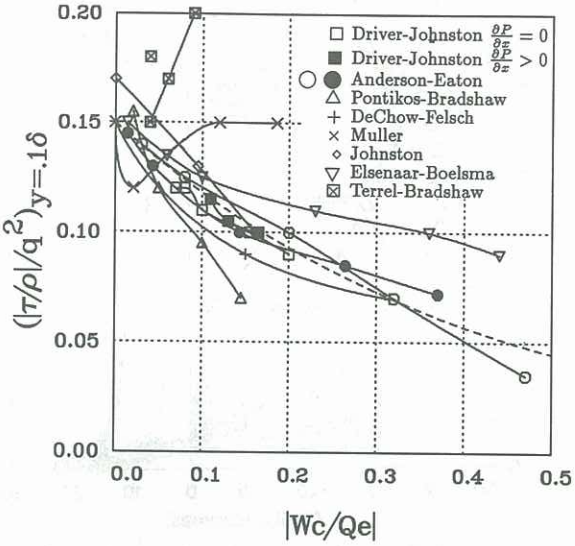

Figure 8 Reynolds stress reduction with cross-flow velocity. $- - - \left(\frac{|\tau/\rho|}{q^2}\right)_{y=.1\delta} = 0.15e^{-2.4\left|\frac{W_c}{Q_c}\right|}$

$\overline{vw}$ Stress Lag Phenomenon

Turbulence, in general, lags in development behind changes in the mean-flow strain field. In particular, the $\overline{vw}$ stress can be seen to lag in responding to changes in $\partial W/\partial y$. This is evident from the evolution of the stress vector direction ($\tan^{-1}\frac{\overline{vw}}{-\overline{uv}}$) which is evaluated along a streamline as shown in Figure 9. Downstream of the spinning section, the mean flow strain-rate vector ($\tan^{-1}\frac{\partial W/\partial y}{\partial U/\partial y}$) turns rapidly toward the mean flow direction (in response to the new boundary condition). However, the stress vector continues to point in the original -45° for some time before eventually turning toward the mean flow direction.

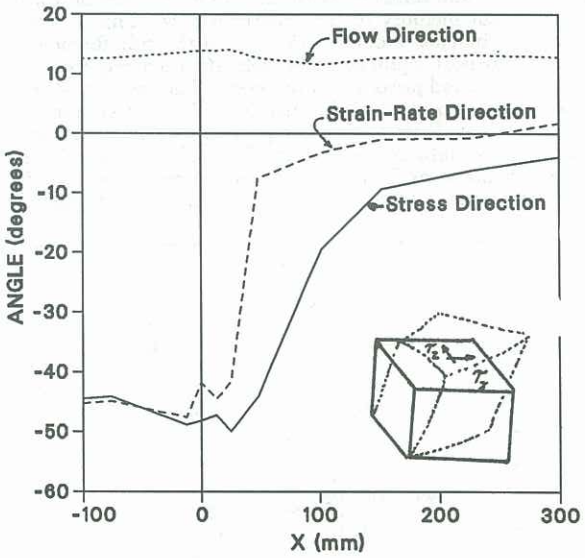

Figure 9 Principal stress and strain-rate directions along ϕ = 3 mm streamline.

The stress vector direction is different from the strain-rate vector direction through the inner half of the boundary layer at the X=152 mm station as shown in Figure 10. This difference in direction is an indication that scalar eddy-viscosity models will be inaccurate at predicting $\overline{vw}$ stress. The Rotta (1979) T-model, predicts this difference between the stress and strain-rate directions, provided a judicious choice of reference frames is used (such as a spinning frame of reference). However, an injudicious choice of reference

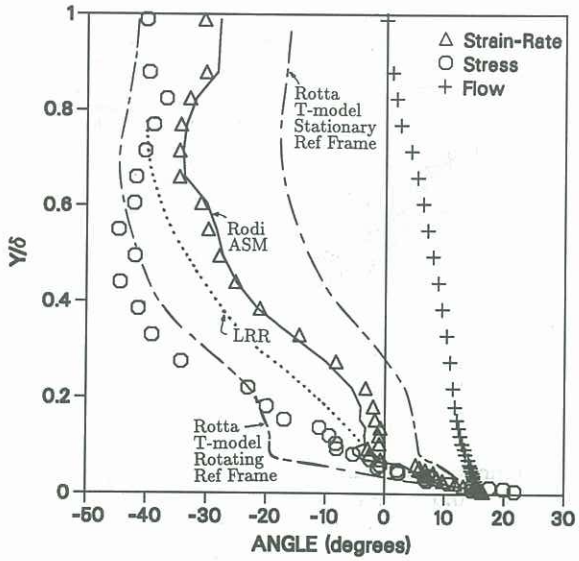

Figure 10 Principal stress and strain-rate direction profile at X=152 mm compared to models.

frames (such as a stationary frame) produces a worse prediction than the eddy-viscosity model. The Rodi (1976) algebraic stress model fails to predict the stress direction any better than an isotropic eddy viscosity model, as indicated by the stress direction being nearly identical to the strain-rate direction. Computations using the Launder, Reece, & Rodi (1975) model produce a better prediction of the stress direction (computational results were adjusted to match the experimental mean flow strain field).

Evaluation of terms in the $\overline{vw}$ stress transport equation reveal the considerable history effects as shown in Figure 11. Terms in the equation were evaluated directly using gradients of the data, except pressure strain, which was deduced from a balance of the equation. The large relative magnitude of the convective term relative to the production, pressure strain, and diffusion is an indication that the flow has a significant memory of the upstream flow. This is what causes turbulence modelers to turn to the full Reynolds-stress transport equations. Models are then required for the diffusion and pressure-strain terms. The pressure-strain model is the most critical, since it is the largest term in the equation. Four models for pressure strain were compared to the data and all but the Shih and Lumley (1985) model (denoted as SL on Fig. 11) under predicted the $\overline{vw}$ pressure strain. Pressure strain models by Naot, Shavit

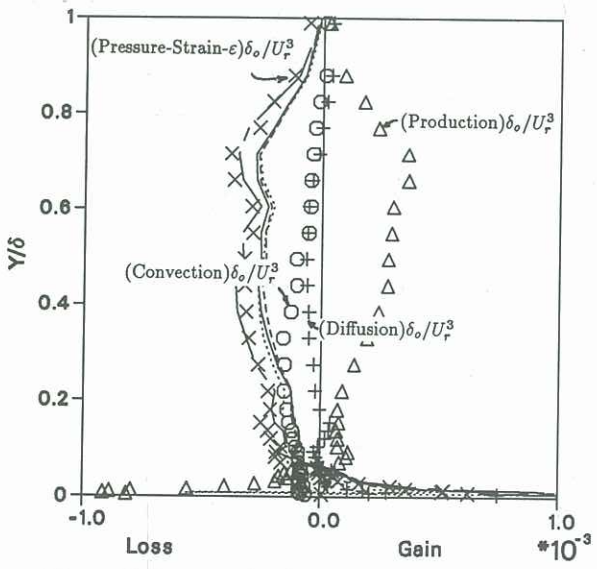

Figure 11 $\overline{vw}$-equation balance at X=152 mm. —— NSW, - - - LRR, ····· FLT, — - — SL.

& Wolfshtein (1973), Launder, Reece, & Rodi (1975), and Fu, Launder, & Tselepidakis (1987) are denoted by NSW, LRR, and FLT, respectively. Despite the improved agreement with the Shih & Lumley model for the spinning case, the agreement is not so good for the non-spinning cases as can be seen in Driver & Johnston (1989).

CONCLUSIONS

An experiment was performed on a three-dimensional turbulent boundary layer subject to adverse pressure gradient, in an effort to provide information for turbulence models. The data indicate that $-\overline{uv}$ Reynolds stress decreases in the presence of transverse strain. The various turbulence models tested were unable to predict the decrease in streamwise stress associated with three-dimensionality. The reduction in stress appears to correlate with the magnitude of the crossflow for this experiment as well as several other experiments in the literature.

The $\overline{vw}$ Reynolds stress was seen to lag in development behind the strain. To some extent the full Reynolds stress turbulence model was able to predict this situation. Balance of the $\overline{vw}$ stress transport equation reveals the nonequilibrium nature of the Reynolds stresses and the reasons for using a full Reynolds stress turbulence model.

The effects of the pressure gradient appear to add linearly to the effects of transverse strain, that is, pressure gradient decreases the Reynolds stress in the vicinity of the wall and mildly increases the stress in the middle of the boundary layer, similar to that of a two-dimensional boundary layer. While transverse strain is believed to reduce a boundary layer's resistance to separation, this could not be directly proved here.

REFERENCES

BRADSHAW, P. and PONTIKOS, N. (1985) Measurements in the Turbulent Boundary Layer on an "Infinite" Swept Wing. Journal of Fluid Mechanics, 159, pp. 105-130.

DRIVER, D.M. and HEBBAR, S.K. (1987) Experimental Study of a Three-Dimensional, Shear-Driven, Turbulent Boundary Layer. AIAA Journal 25, pp. 35-42.

DRIVER, D.M. and JOHNSTON, J.P. (1989) Experimental Study of a Three-Dimensional, Shear-Driven, Turbulent Boundary Layer with Streamwise Adverse Pressure Gradient. NASA TM-102211, October 1989.

FU, S., LAUNDER, B.E., and TSELEPIDAKIS, D.P. (1987) Accommodating the Effects of High-Strain Rates in Modeling the Pressure-Strain Correlation. University of Manchester, Mechanical Engineering Department, Report TFD/87/5.

LAUNDER, B.E., REECE, G.J. and RODI, W. (1975) Progress in the Development of a Reynolds-Stress Turbulence Closure. Journal of Fluid Mechanics, 68, pp. 537-566.

NAOT, D., SHAVIT, A., and WOLFSHTEIN, M. (1973) Two-Point Correlation Model and the Redistribution of Reynolds Stresses. Physics of Fluids, 16, pp. 738-743.

RODI, W. (1976) A New Algebraic Relation for Calculating Reynolds Stresses. Zeitschrift fuer Angewandte Mathematik und Mechanik, 56, pp. 219-221.

ROTTA, J.C. (1979) A Family of Turbulence Models for Three-Dimensional Boundary Layers. Turbulent Shear Flows Conference, VOL. II, Springer-Verlag, New York.

SHIH, T-H. and LUMLEY, J.L. (1985) Modeling of Pressure Correlation Terms in Reynolds Stress and Scalar Flux Equations. Report FDA-85-3, Sibley School of Mechanical and Aerospace Engineering, Cornell University.

SIMPSON, R., CHEW, Y., and SHIVAPRASAD, B. (1981) The Structure of a Separating Turbulent Boundary Layer. Part 1. Mean Flow and Reynolds Stresses. Journal of Fluid Mechanics, 113, pp. 23-51.

WILCOX, D.C. and RUBESIN, M.W. (1980) Progress in Turbulence Modeling for Complex Flow Fields Including the Effect of Compressibility. NASA TP-1517.